Fault Detection and Localization in LV Smart Grids

Nikolaos Sapountzoglou, Bertrand Raison, Nuno Silva

Fault Detection and Localization in LV Smart Grids

Nikolaos Sapountzoglou
Univ. Grenoble Alpes, CNRS, Grenoble INP, G2Elab
38000 Grenoble, France
nikolaos.sapountzoglou@g2elab.grenoble-inp.fr

Bertrand Raison
Univ. Grenoble Alpes, CNRS, Grenoble INP, G2Elab
38000 Grenoble, France
bertrand.raison@g2elab.grenoble-inp.fr

Nuno Silva
Efacec
Maia, Portugal
nuno.silva@efacec.com

***Abstract*—In this paper, a fault detection and localization method for a Low Voltage (LV) distribution grid are presented. Two fault detection approaches were examined both suitable only for low impedance faults (up to 10 Ω of fault resistance). The first one was based on current measurements at the beginning of the feeder and the second one was based on the highest voltage drop across the feeder branches. The localization method was based solely on nodal rms voltage measurements across the grid. The localization method was divided in three steps: a) faulty branch identification, b) faulty sector localization and c) fault distance estimation. Two categories of faults were examined: single-phase to ground short-circuit (SC) faults and three-phase SC faults. Faults were divided in two major categories: a) faults in the beginning of a branch and b) faults in the middle or towards the end of a branch. Additionally, in order to study the effects of loads and microgeneration units, four different hours in a day were chosen. For all of the above cases both low and high impedance faults were studied with fault resistance values ranging from 0.1 Ω to 1 $k\Omega$. Finally, a preliminary study with less available measurements was made and presented in this paper. The results have been validated by simulation means on a real semi-rural LV distribution network of Portugal.**

***Index Terms*—fault detection, fault location, LV smart grids**

I. Introduction

Faults in a typical distribution grid are responsible for 80% of customer interruptions [1]. The most popular index to monitor the reliability of a distribution grid is the system average interruption duration index (SAIDI). In 2016, among the European countries, the unplanned SAIDI including excepetional events ranged from 9 min (Switzerland) to 371 min (Romania) per customer [2].

The increased penetration of distributed generators such as photovoltaic (PV) systems in distribution grids has increased their complexity. In the context of the evolution of smart grids as the necessary tool to tackle those challenges, safe operation and fault location are the first steps towards a self-healing power system. These functionalities will help reduce the outage time and increase the lifetime of the grid elements and at the same time reduce the operational cost of the network and increase its reliability.

The available fault localization techniques in literature can be divided in five big categories: a) impedance based methods (the most popular), b) knowledge based methods (mostly artificial intelligence), c) traveling wave methods, d) methods based on sparse measurements (mainly voltage but also current) and e) hybrid methods which combine two or more of the above methods. Some of the most popular of those approaches are cited below.

Being probably the most explored approach to localize faults in distribution grids, impedance based methods, account for a large number of published papers. An iterative approach to estimate the loads and the fault current at each line section was accompanied by a load variation and fault resistance sensitivity analysis in [3]. In [4], a π line model was used to improve the accuracy of the method for a power distribution network with integrated PV systems; the results were validated on a real test feeder simulator. Another attempt to enhance the accuracy of the classical impedance based method, was made in [5] through the use of voltage measurements obtained from smart meters. Finally, in [6] the current contribution of the inverter-interfaced PV to the fault, was taken into account in the estimation of the fault location.

Other researchers used knowledge based methods. A combination of sparse representation vector, fuzzy-clustering and machine learning techniques to estimate the fault distance for single faults and for double or triple faults occurring simultaneously was investigated in [7]. Furthermore, decision trees were developed in order to identify the faulty segment of the grid before localizing the faulty node [8]. An alternative option would be to train two neural networks to identify the type of the occurring fault as well as its location as explained in [9]. Moreover, a fault detection and identification method based on hidden Markov models along with a location method based on matching pursuit decomposition for the feature extraction from voltage signals, were proposed in [10].

As far as traveling wave methods are concerned, integrated time-frequency wavelet decomposition of the voltage transients combined with the traveling waves originating from the fault, were implemented in [11] to estimate the fault location. Their results were validated through measurements from a real MV distribution network. In [12], the digital wavelet transform (DWT) was used together with a global position system clock to estimate the fault distance from the busbars.

The last big category of fault localization methods is the one based on sparse measurements. Smart meters have been used to measure pre-fault and fault voltages and from them

This project has received funding from the European Union's Horizon 2020 research and innovation programme under the Marie Skłodowska-Curie grant agreement No 675318 (INCITE).

produce a current vector which would present only one nonzero element. The latter corresponded to the bus under fault [13]. In [14], sparse voltage measurements were used to analyze propagating voltage sags for each feeder node during a fault. Similarly, in a method that matches calculated voltage sags with acquired voltage data from nodal measurements is presented in [15]. Furthermore, in the emerging context of smart grids, new functionalities for the detection and location of a fault are becoming available in the LV grid [16]. Additionally, a fault detection and localization approach for non-technical losses is presented in [17]. A method taking advantage of both voltage and current measurements at the interconnection points of distributed generation units to form a general method for fault location was proposed in [18]. On the other hand, the method described in [19] was solely based on current measurements. The method uses the phase current angles and the amplitudes of zero-sequence node currents to localize the fault.

A promising field that seems to attract a lot of attention lately is the one of hybrid methods. Two recent studies demonstrated the potential of using elements from different methods to improve the estimation accuracy. In [20] a combination of DWT and artificial neural networks was used to identify the faulty section of the network and locate the fault. In [21] a fault detection and location approach based on mathematical morphology and the recursive least-square method was investigated for the case of microgrids.

Besides the promising results that the above methods may present, the vast majority of the studies in literature were focused on low-impedance faults with fault resistance values between 5 $m\Omega$ and 50 Ω. Only very few investigated high-impedance fault cases [6], [22]. In addition, up until now and probably because of the complexity they present and the absence of available measurements, there has not been a lot of research around LV distribution grids. A few studies can be found in [5], [16], [17], [19]. The rest of the studies have examined the MV distribution grid. On top of these, impedance methods present a very specific and important disadvantage: they identify multiple locations as candidates for fault occurrence.

In an attempt to shed light in a quite unexplored field, a fault detection and a fault localization method are proposed for both low and high-impedance faults in LV distribution grids in this paper; the method was tested for a broad range of fault resistance values ranging from 0.1 Ω to 1000 Ω. Additionally, both single-phase to ground and three-phase faults were studied. In a distribution system, 70% of the faults are single-phase to ground faults and only 5% three-phase [1]. However, three-phase faults are the most severe. By selecting those two types, the most frequent and most severe faults were studied. The basic idea of the fault localization method was initially presented in [22] for MV distribution networks but in this case it was adapted and tested in a real LV grid.

The structure of the paper is as follows. In the next Section the characteristics of the grid under study are presented. In the third Section the fault detection approach is discussed. The fourth Section thoroughly describes the developed methodology and the obtained results are presented in the fifth Section. Finally, the conclusions are summarized the last Section along with some proposals for future work.

II. Grid

The topology of the studied LV distribution grid along with the available sensors are presented in Fig. 1; its a three-phase-four-wire grid with a solidly grounded neutral. The grid is both unbalanced and heterogeneous. Unbalanced since the different loads and microgeneration units, in this case PV systems, are of different size and both of them connected through a single-phase to the grid; heterogeneous because lines connecting the nodes are of different resistance, reactance and length. It was assumed that the measurements were synchronized and accurate.

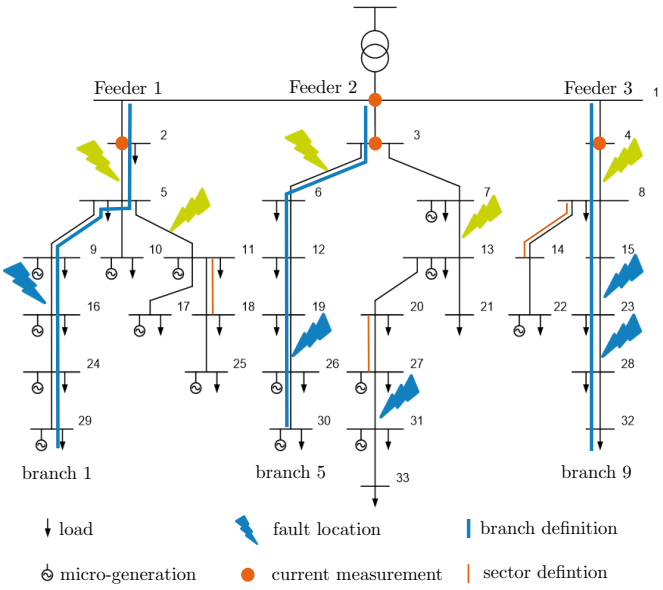

Fig. 1: Single line diagram of the LV grid with the SC fault cases. Two categories of faults are presented: a) faults close to the beginning of the feeder (green symbols) and b) faults towards the middle of the end of the feeder (blue symbols).

III. Fault Detection

An attempt to detect faults was made in this study. Two approaches were examined: one solely based on the rms value of the current at the beginning of each feeder and another based on the voltage drop across the faulty feeder. In both approaches a faulty phase discrimination was implemented as well. Faults were studied in their steady state, 150 ms after their occurrence; a time fast enough for the protective elements to isolate the PVs as this was expected to happen around 200 ms.

For the first approach, current sensors were placed at the beginning of each feeder (Fig. 1). Theoretically, at the moment of a fault occurrence a sudden increase of the current is expected. An example of this sudden increase is provided in Table I. The influence of the fault resistance on the increase of

TABLE I: Current increase at feeder level for a single-phase to ground SC fault (CG) between nodes 15 and 23 at $20h01m0.15s$ (steady-state) for different fault resistance values.

$R_f(\Omega)$	0.1	1	5	10	50	100	500	1000
$I(pu)$	24.9	9.3	3.1	2.1	1.21	1.11	1.02	1.01

the current is clearly depicted: the higher the fault resistance, the smaller the current increase under faulty operation will be. For fault resistance values higher than 50 Ω the fault current is slightly higher than normal operation. This last observation lead to the conclusion that for high fault resistance values (higher than 50 Ω) faults cannot be easily detected based only on the rms value of the current at the beginning of the feeder level.

For the second approach, the voltage sensors of Fig. 1 were used. In theory, after a fault occurrence a voltage drop is expected. According to the EN50160 standards in LV grids, only a voltage drop higher than 10% of the one under normal operating conditions is considered as an anomaly. For the same fault case as the one demonstrated in Table I, the voltage profiles across the faulty branch are presented in Fig. 2 expressed in the per unit scale for different fault resistance values. It can be easily noticed that a 5 Ω fault resistance value fault marginally passes the threshold of 10%. Faults with fault resistance higher than 5 Ω fall into the permitted by the EN50160 standards voltage drop zone. Only the detection of faults with 0.1 and 1 Ω are guaranteed.

Since neither of the two methods can guarantee the detection of high impedance faults, the development of other tools is necessary. For the rest of this study, the detection of the fault and more specifically of the identification of the faulty feeder was considered as being successful and its localization is investigated in the following Section.

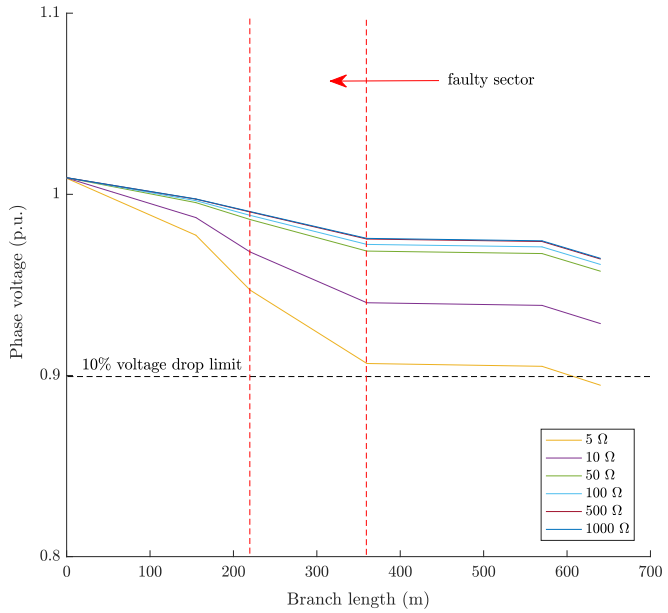

Fig. 2: Snapshot of voltage profile for a single-phase to ground SC fault (CG) between nodes 15 and 23 at $20h01m0.15s$.

IV. Fault Localization Method

After the detection of a fault on a specific feeder, a three-step method was applied to estimate the fault location as presented in Fig. 3: a) identify the faulty branch, b) localize the faulty sector and c) estimate the distance of the fault from the beginning of the feeder. As mentioned in the Introduction the method was based on the available nodal rms voltage phase measurements. Phase voltage values were used for the case of single-phase to ground faults while a symmetrical component analysis of the voltage (positive, negative and zero sequence components) lead to the choice of the positive sequence component of voltage as more suitable for the case of three-phase faults.

As presented in Fig. 1, two different categories of faults were considered in terms of their location: a) faults in the beginning of the feeder and b) faults towards the middle or the end of a branch. Faults in the beginning of the feeder might belong to multiple branches as is the case of the one between nodes two and five which belongs to all four branches of the first feeder. After a comparative analysis, for faults in

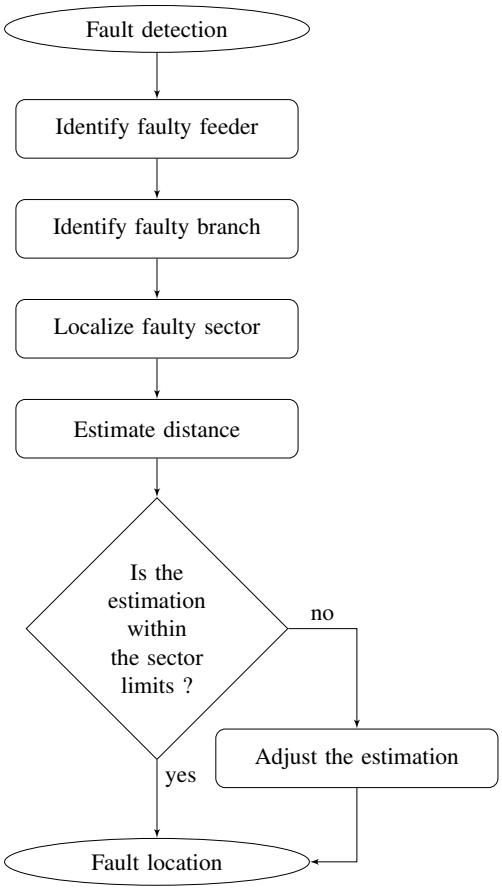

Fig. 3: Fault localization method flowchart

the beginning of the feeder, it was found that depending on the phase in which the fault was present, the branch with the less elements (loads or microgeneration) connected to that phase should be chosen to obtain the voltage profile. Although the method performs well if the correct branch is identified, this is a very challenging task as quite often the wrong branch would be found as the one under fault. The results presented in this paper focus on the second category of faults: faults located towards the middle or the end of the branch.

In an attempt to solve the problem described above (faults located in the beginning of the feeder), an alternative approach was investigated in identifying the faulty branch. Instead of searching for the branch to which the node with the minimum voltage belongs, a step by step comparison of the available measurements within each branch of the same feeder was implemented as described in Algorithm 1.

Once the faulty branch has been identified the two final steps of the method were initiated. As presented in Fig. 2 the basic idea of the faulty sector localization process lies in the fact that after the sector where the fault occurred, a stabilization of the voltage profile curve with a zero slope was expected. The latter is theoretically explained by the fact that after that point there should be no circulating current (for zero fault resistance) or a fixed amount (for non zero fault resistance). Furthermore, an extrapolation of the lines adjacent to the faulty sector was used and their intersection indicated the fault location. The analytical algorithm for the faulty sector localization and the distance estimation is presented in Algorithm 2. Finally, the distance estimation error was calculated using the following equation [23]:

$$error(\%) = \frac{|d_{estimated} - d_{actual}|}{l_{total}} \cdot 100 \qquad (1)$$

where l_{total} is the total branch length.

V. Results

A total of five influencing parameters were analyzed: a) location of the fault inside the feeder (close to the beginning or further away), b) load and microgeneration penetration levels (four different scenarios during a day presented in Table II), c) fault resistance value (eight different values were considered: 0.1, 1, 5, 10, 50, 100, 500 and 1000 Ω), d) the type of the fault (single-phase and three-phase faults) and e) the available voltage measurements. One top of those, the unbalanced and heterogeneous nature of the grid should be again underlined. Finally, a global simultaneity factor of 30% was used for the loads of the grid. The results are presented below.

A. Faulty Branch Identification: Horizontal vs. Vertical Approach

The horizontal method was found to be 9% more efficient than the vertical one in identifying the faulty branch for faults located at the beginning of the feeder but equally less efficient for faults in the middle or the end of the branch. Considering this trade off, the vertical method was chosen as it is easier in real life to localize faults in the beginning of the feeder.

Algorithm 1 Fault Localization Algorithm - Step I

procedure FAULTY BRANCH IDENTIFICATION - VERTICAL
    within a faulty feeder
    $min\_v \leftarrow min\_v(faulty\_feeder)$
                                ▷ *br: branch*
    for $i = first\_br : last\_br$ **do**
        if $v(i) = min\_v$ **then**
            $faulty\_br \leftarrow i$

procedure FAULTY BRANCH IDENTIFICATION - HORIZONTAL
    within a faulty feeder
                                ▷ *msp: measurement point*
    for $j = first\_msp + 1 : last\_msp$ **do**
        $min\_count \leftarrow 0$
        $min\_v2 \leftarrow min(v(first\_br : last\_br, j))$
        for $i = first\_br : last\_br$ **do**
            if $v(i, j) = min\_v2$ **then**
                $min\_count \leftarrow min\_count + 1$
                if $min\_count = 1$ **then**
                    $faulty\_br \leftarrow i$
        if $min\_count = 1$ **then**
            $break$

Algorithm 2 Fault Localization Algorithm - Step II

procedure FAULTY SECTOR LOCALIZATION
    accross the faulty branch
                                ▷ *msp: measurement point*
    for $i = first\_msp + 1 : last\_msp$ **do**
        $\delta v(i) \leftarrow v(i) - v(i-1)$
    $fs \leftarrow 0$ ▷ *fs: faulty sector*
    $min\_v3 \leftarrow min(|\delta v|)$
                                ▷ *first voltage criterion*
    for $i = first\_msp + 1 : last\_msp$ **do**
        if $fs = 0$ **and** $\delta v(i-1) < 0$ **and** $\delta v(i) > 0$ **then**
            $fs \leftarrow i - 1$
            $break$
                                ▷ *second voltage criterion*
    for $i = first\_msp : last\_msp - 1$ **do**
        if $fs = 0$ **and** $|\delta v(i)| = min\_v3$ **then**
            $fs \leftarrow i - 1$
            $break$

procedure DISTANCE ESTIMATION
    extrapolation of the lines of the adjacent sectors
    calculation of their intersection point
    $d_{est} \leftarrow$ *distance corresponding to the intersection point*
    if $d_{est} > fs\_upper\_limit$ **then**
        $d_{est} \leftarrow fs\_upper\_limit$
    else if $d_{est} < fs\_lower\_limit$ **then**
        $d_{est} \leftarrow fs\_lower\_limit$
    fault location at $d_{est}(m)$ from the beginning of the feeder

B. Faulty Sector Localization and Distance Estimation

Failing to identify the correct sector under fault can lead to a direct increase of the error of distance estimation. In the vast majority of sector mislocalization cases, an adjacent sector was found as the one under fault. This, of course increased the estimation error. It is derived from Table III that the method presented higher accuracy in three phase faults than in single-phase to ground faults. It is also obvious that by increasing the fault resistance the distance estimation error increases.

C. Fault Resistance Sensitivity Analysis

From Table III it is clear that for faults of a fault resistance of less than 50 Ω the precision of the method in identifying the correct branch and sector is significantly increased by 16.67% and 23.21% respectively for single-phase faults and by 25% and 12.5% for three-phase faults. This means that by increasing the fault resistance mislocalizations of faulty branches and sectors are to be expected.

The above phenomenon was attributed to the fact that by increasing the fault resistance, the voltage profile approaches the one at normal operating conditions and thus the micro-generation and load effects on the voltage profile were more severe.

D. Less Available Measurements

A preliminary analysis of less available measurements was made for single-phase to ground SC faults in two different locations: a) between nodes nine and sixteen and b) between nodes nineteen and twenty six of Fig 1; faults in all three phases were implemented for both cases. In order to establish some criteria for a sensor placement strategy, some ideas were drawn from a state estimation example in [24]. There, the authors mention that sensors should be placed: a) in nodes where big loads are connected, b) towards the end of the feeder and c) in branches with large current being transported. However, since the fault localization method presented in this paper is solely based on the voltage curve along a faulty branch, a few modifications in the selection criteria were made. A limitation of the method is that it needs at least three distinct sectors in order to work, meaning a minimum of four measurements per branch; at least the first and the last two. In order to establish the placement criteria, the following scenarios were tested for each of the aforementioned fault cases for all three phases:

[f1] fault between nodes nine and sixteen
- i) sensors in nodes: 1, 2, 24 and 29
- ii) sensors in nodes: 1, 2, 16, 24 and 29
- iii) sensors in nodes: 1, 2, 9, 24 and 29

[f2] fault between nodes nineteen and twenty six
- i) sensors in nodes: 1, 3, 26 and 30
- ii) sensors in nodes: 1, 3, 19, 26 and 30
- iii) sensors in nodes: 1, 3, 12, 26 and 30

For both fault cases, the scenario of retaining the bare minimum of four required measurements was rejected due to a significant increase of the error in distance estimation. Consequently, the addition of an extra measurement in between the first two (beginning of the branch) and the last two (end of the branch) was deemed necessary. Scenarios (iii) presented the best performance for both cases. Their distance estimation accuracy results are presented in Table IV in comparison to the ones obtained with available measurements at every node; an increase of the distance estimation error of 12.05% and 5.82% was noticed for the first and second case respectively.

The choice of scenario (iii) for the first case can be justified since node nine presents two characteristics: a) it has loads connected in all three phases accumulating more power than the ones connected in nodes five or sixteen and b) is a measurement in the middle of nodes two and twenty four which will lead to a voltage curve approximation closer to the one with full measurements. For the second fault case (f2), scenario (iii) performed better than (ii) because although both nodes twelve and nineteen had the same load characteristics, node twelve was located in the middle of nodes three and twenty six thus providing a better approximation of the voltage curve.

Based on the above analysis, the following strategy of sensor placement was developed: a) voltage sensors should be spread throughout the branch (a minimum of the first two and the last two is required) so that the voltage curve would be a good approximation of the ideal case and b) nodes with big loads and/or microgeneratiion units connected to them should be prioritized taking into account all three phases. To summarize, with a reduction 30% of the available measurements (two from the first branch and two from the fifth branch) for the two studied fault cases, an increase of approximately 10% of the distance estimation error was noticed maintaining an accuracy of distance estimation higher than 81%.

TABLE II: Simulation scenarios

	Time	Microgeneration	Load
1	01:00	0%	28%
2	20:00	0%	90%
3	14:00	49%	60%
4	12:00	100%	50%

TABLE III: Method accuracy (%)

	Overall		Less than 50 Ω	
	1 ph	3 ph	1 ph	3 ph
branch	75.00	75.00	91.67	100.0
sector	58.61	87.50	81.82	100.0
distance	89.33	95.21	93.11	96.03

TABLE IV: Distance estimation error (%) of single-phase to ground faults for the cases of less available measurements in the grid.

	Normal	Less measurements
[f1] 9-16, scenario iii	6.80	18.85
[f2] 19-26, scenario iii	8.50	14.32

VI. Conclusions and Future Works

In this paper, two fault detection detection approaches and a fault localization algorithm with two methods of faulty branch identification were developed for LV smart grids. Additionally, a sensor placement strategy was proposed based on preliminary results. A real semi-rural LV distribution network of Portugal was used for the simulations.

Six influencing factors were taken into account: a) the unbalanced and heterogeneous nature of the grid, b) faults in different locations: in the beginning of the feeder and in the middle or towards the end of the branch, c) different types of faults: single-phase to ground and three-phase, d) different scenarios of load and microgeneration penetration percentages, e) different fault resistance values ranging from 0.1 Ω to 1000 Ω and f) less available voltage sensors.

With an overall accuracy in fault distance estimation of 89.33% for single-phase to ground faults and 95.21% for three-phase faults under all the aforementioned different operating conditions the method was found to be a reliable solution for fault localization in LV smart grids.

The main conclusions are summarized below:

- Both fault detection approaches were found to be reliable only for low impedance faults
- For the faulty branch identification, the horizontal approach was more suitable for faults located close to the beginning of the feeder while the vertical for the rest.
- Positive sequence component of the voltage was considered as the most suitable for three-phase faults.
- The method was more successful for three-phase faults and especially in low impedance ones where the method presented 100% success in identifying the faulty branch and sector and 3.97% of error in estimating the fault distance. This was attributed to the fact that the behavior of the components in all three phases was taken into account.
- While fault resistance increases the accuracy decreases.
- The localization method requires voltage sensors spread across the length of the branch. Nodes with big loads or microgeneration should be prioritized.

Future work would extend and finalize the less available measurements study for the whole grid and include uncertainty of measurements in the fault localization algorithm.

References

[1] T. Gönen and T. Gönen, *Electric Power Distribution Engineering*. Boca Raton, FL: CRC Press, 2014, oCLC: 879683602.

[2] CEER, "6th Benchmarking Report on the Continuity of Electricity and Gas Supply," Brussels, Tech. Rep. C 18 - EQS - 86 - 03, 2016.

[3] S.-J. Lee, M.-S. Choi, S.-H. Kang, B.-G. Jin, D.-S. Lee, B.-S. Ahn, N.-S. Yoon, H.-Y. Kim, and S.-B. Wee, "An intelligent and efficient fault location and diagnosis scheme for radial distribution systems," *IEEE Transactions on Power Delivery*, vol. 19, no. 2, pp. 524–532, Apr. 2004.

[4] R. Dashti, M. Ghasemi, and M. Daisy, "Fault location in power distribution network with presence of distributed generation resources using impedance based method and applying π line model," *Energy*, vol. 159, pp. 344–360, Sep. 2018.

[5] F. C. L. Trindade and W. Freitas, "Low Voltage Zones to Support Fault Location in Distribution Systems With Smart Meters," *IEEE Transactions on Smart Grid*, vol. 8, no. 6, pp. 2765–2774, Nov. 2017.

[6] C. Orozco-Henao, A. S. Bretas, A. R. Herrera-Orozco, J. D. Pulgarín-Rivera, S. Dhulipala, and S. Wang, "Towards active distribution networks fault location: Contributions considering DER analytical models and local measurements," *International Journal of Electrical Power & Energy Systems*, vol. 99, pp. 454–464, Jul. 2018.

[7] M. Majidi, M. Etezadi-Amoli, and M. S. Fadali, "A Novel Method for Single and Simultaneous Fault Location in Distribution Networks," *IEEE Transactions on Power Systems*, vol. 30, no. 6, pp. 3368–3376, Nov. 2015.

[8] Y. Dong, C. Zheng, and M. Kezunovic, "Enhancing Accuracy While Reducing Computation Complexity for Voltage-Sag-Based Distribution Fault Location," *IEEE Transactions on Power Delivery*, vol. 28, no. 2, pp. 1202–1212, Apr. 2013.

[9] M. Sarvi, "Determination of Fault Location and Type in Distribution Systems using Clark Transformation and Neural Network," *International Journal of Applied Power Engineering (IJAPE)*, vol. 1, no. 2, Aug. 2012.

[10] H. Jiang, J. Zhang, W. Gao, and Z. Wu, "Fault Detection, Identification, and Location in Smart Grid Based on Data-Driven Computational Methods," *Smart Grid, IEEE Transactions on*, vol. 5, pp. 2947–2956, Nov. 2014.

[11] A. Borghetti, M. Bosetti, C. A. Nucci, M. Paolone, and A. Abur, "Integrated Use of Time-Frequency Wavelet Decompositions for Fault Location in Distribution Networks: Theory and Experimental Validation," *IEEE Transactions on Power Delivery*, vol. 25, no. 4, pp. 3139–3146, Oct. 2010.

[12] H. Nouri, C. Wang, and T. Davies, "An accurate fault location technique for distribution lines with tapped loads using wavelet transform," in *2001 IEEE Porto Power Tech Proceedings (Cat. No.01EX502)*, vol. 3, Sep. 2001, pp. 4 pp. vol.3–.

[13] M. Majidi, A. Arabali, and M. Etezadi-Amoli, "Fault Location in Distribution Networks by Compressive Sensing," *IEEE Transactions on Power Delivery*, vol. 30, no. 4, pp. 1761–1769, Aug. 2015.

[14] R. A. F. Pereira, L. G. W. da Silva, M. Kezunovic, and J. R. S. Mantovani, "Improved Fault Location on Distribution Feeders Based on Matching During-Fault Voltage Sags," *IEEE Transactions on Power Delivery*, vol. 24, no. 2, pp. 852–862, Apr. 2009.

[15] S. Lotfifard, M. Kezunovic, and M. J. Mousavi, "Voltage Sag Data Utilization for Distribution Fault Location," *IEEE Transactions on Power Delivery*, vol. 26, no. 2, pp. 1239–1246, Apr. 2011.

[16] N. Silva, F. Basadre, P. Rodrigues, M. S. Nunes, A. Grilo, A. Casaca, F. Melo, and L. Gaspar, "Fault detection and location in Low Voltage grids based on distributed monitoring," in *2016 IEEE International Energy Conference (ENERGYCON)*, Apr. 2016, pp. 1–6.

[17] L. Marques, N. Silva, I. Miranda, E. Rodriges, and H. Leite, "Detection and localisation of non-technical losses in low voltage distribution networks," in *Mediterranean Conference on Power Generation, Transmission, Distribution and Energy Conversion (MedPower 2016)*, Nov. 2016, pp. 1–8.

[18] S. M. Brahma, "Fault Location in Power Distribution System With Penetration of Distributed Generation," *IEEE Transactions on Power Delivery*, vol. 26, no. 3, pp. 1545–1553, Jul. 2011.

[19] G. Niu, L. Zhou, W. Pei, and Z. Qi, "A novel fault location and recognition method for low voltage active distribution network," in *2015 5th International Conference on Electric Utility Deregulation and Restructuring and Power Technologies (DRPT)*, Nov. 2015, pp. 876–881.

[20] A. C. Adewole, R. Tzoneva, and S. Behardien, "Distribution network fault section identification and fault location using wavelet entropy and neural networks," *Applied Soft Computing*, vol. 46, pp. 296–306, Sep. 2016.

[21] T. Gush, S. B. A. Bukhari, R. Haider, S. Admasie, Y.-S. Oh, G.-J. Cho, and C.-H. Kim, "Fault detection and location in a microgrid using mathematical morphology and recursive least square methods," *International Journal of Electrical Power & Energy Systems*, vol. 102, pp. 324–331, Nov. 2018.

[22] A. Teninge, C. Pajot, B. Raison, and D. Picault, "Voltage profile analysis for fault distance estimation in distribution network," in *2015 IEEE Eindhoven PowerTech*, Jun. 2015, pp. 1–5.

[23] M. M. Saha, J. Izykowski, and E. Rosołowski, *Fault Location on Power Networks*, ser. Power systems. London: Springer, 2010, oCLC: ocn495597133.

[24] M. Picallo, A. Anta, B. D. Schutter, and A. Panosyan, "A Two-Step Distribution System State Estimator with Grid Constraints and Mixed Measurements," in *2018 Power Systems Computation Conference (PSCC)*, Jun. 2018, pp. 1–7.